Effect of resource constraints on intersimilar coupled networks

S. Shai* and S. Dobson

School of Computer Science, University of St. Andrews, Jack Cole Building, North Haugh, St. Andrews, Fife KY16 9SX, Scotland, UK

(Received 14 February 2012; revised manuscript received 4 October 2012; published 28 December 2012)

Most real-world networks do not live in isolation but are often coupled together within a larger system. Recent studies have shown that intersimilarity between coupled networks increases the connectivity of the overall system. However, unlike connected nodes in a single network, coupled nodes often share resources, like time, energy, and memory, which can impede flow processes through contention when intersimilarly coupled. We study a model of a constrained susceptible-infected-recovered (SIR) process on a system consisting of two random networks sharing the same set of nodes, where nodes are limited to interact with (and therefore infect) a maximum number of neighbors at each epidemic time step. We obtain that, in agreement with previous studies, when no limit exists (regular SIR model), positively correlated (intersimilar) coupling results in a lower epidemic threshold than negatively correlated (interdissimilar) coupling. However, in the case of the constrained SIR model, the obtained epidemic threshold is lower with negatively correlated coupling. The latter finding differentiates our work from previous studies and provides another step towards revealing the qualitative differences between single and coupled networks.

DOI: 10.1103/PhysRevE.86.066120 PACS number(s): 89.75.Fb, 89.75.Hc

I. INTRODUCTION

In the past decade the structure and dynamics of complex networks have been widely investigated and used as a framework for studying complex systems where nodes are the entities and links are the relations between them. While most studies until now have focused on isolated single networks that do not interact with or depend on other networks, recent studies suggest various coupled-network models, including the layered model [1], interdependent networks [2], interacting networks [3], and multiplex networks [4].

Recently the effects of nonrandom coupling between nodes in a system of coupled networks have been examined. The term *intersimilarity* was coined by Parshani *et al.* [5] to describe the case where nodes are coupled according to some regularity. They consider two types of intersimilarity: the inter-degree-degree correlation corresponds to the coupling of nodes of a similar degree, and the interclustering coefficient corresponds to the coupling of neighbors of coupled nodes. They show that higher intersimilarity, obtained either by a higher inter-degree-degree correlation or by a higher interclustering coefficient, increases the robustness of the network to random failures. Cho *et al.* [6] consider a system of two coupled networks sharing the same set of nodes, called a *multiplex*. They use the Spearman rank correlation coefficient of the degrees of a node in either network as a measure of the internetwork similarity. They show that the giant component emerges earlier with positive correlated coupling, but it grows more gradually than in the case of a negative correlation. Buldyrev *et al.* [7] studied the percolation process on correspondently coupled networks, where mutually dependent nodes have the same number of intranetwork connectivity links. They found that the percolation threshold for correspondently coupled networks is always lower than the one for randomly coupled networks with the same degree distribution. These studies suggest that intersimilarity between coupled networks increases the connectivity of the overall system, thus enhancing the spreading of flows in the system.

However, unlike connected nodes in a single network, coupled nodes often share limited resources, and this will clearly affect any flow process operating over the network. This is obviously the case where the coupled nodes represent the *same* entity, as in a multiplex, but it is also true in the case where the coupled nodes represent *different* entities that interact with or depend on each other. The coupled nodes play a "role" in more than one network and typically have limited resources available. For example, in the case where an overlay node in a communication network is coupled with a router through a physical device (i.e., a host computer), the router's packet queue handles both the packets that are routed to the host and those in the network layer that do not intersect with the host. Counterintuitively it might be better to couple a central overlay node with a noncentral router, so that the router is "dedicated" to the overlay node and is not being heavily loaded with routing general network packets. Similarly, in the case where a person is involved in more than one social network through different types of social links, the person shares his or her time between contacts in different social groups and thus might not be able to play a central role in spreading (for example) news equally among all the different social groups.

It is also worth mentioning that in the work discussed earlier [6], Cho *et al.* studied two coupled real-world networks: one in which proteins are connected through both physical bindings and sharing of metabolites and another in which countries are connected through commodity trades and industrial sectors. The Spearman rank correlation coefficient of the degrees of a node in either network, which is used as a measure of intersimilarity, was 0.86 for the trade relations network, while the measure obtained for the protein network was only 0.11. The authors also show that the protein network behaves similarly to its randomized version (obtained by randomly shuffling the node identities in the two layers), while the world trade network behaves similarly to its positively correlated version (obtained by ordered-matching of degree ranks in the two layers). Our work suggests that a weaker intersimilarity

*saray@cs.st-andrews.ac.uk

between coupled biological networks might also originate due to resource-limitation effects, for example, constrained energy.

In this paper we study a variation of the susceptible-infected-recovered (SIR) epidemic spreading model in a multiplex consisting of two random networks sharing the same set of nodes (also called a *duplex*) where infected nodes can pass the disease to their neighbors in both networks until they recover. The SIR model is a well-established model, and one of the best-studied models in epidemiology [8]. It describes diseases such as human papillomavirus, seasonal influenza, and H1N1 [8,9], as well as rumor spreading [10,11] and the spread of computer viruses [12]. In the model each node exists in one of three discrete states: susceptible (S), infected (I), or recovered (R). Starting with a network of susceptible nodes and introducing a seed of infected nodes, at each time step, each susceptible (healthy) node is infected at infection rate λ if it is connected to one or more infected nodes. At the same time, infected nodes recover at recovery rate μ, after which they are immune to further infection. A multiplex is a coupled-network model describing a network with more than one type of link connecting the nodes [4,13]. Examples include people interacting through different social links (e.g., family, work), proteins interacting through physical bindings and by sharing metabolites in reactions catalyzed by two enzymes, and countries interacting through financial and political channels ranging from commodity trade to political alliance [4].

The variation of the regular SIR model we consider is the introduction of the constraint that nodes are constrained to interact with (and therefore potentially infect) a maximum number of their neighbors at each epidemic time step. This is equivalent to the case whereby a person can only meet a certain number of his or her friends in a period of time: it seems clear that in the case of frequency-dependent processes (such as for sexually transmitted diseases [14]), such contact limitations will potentially affect the spread of the disease through the network. We present the results of extensive simulations of both constrained and regular SIR epidemics spreading on a duplex consisting of two Erdős-Rényi (ER) [15] or Barabási-Albert (BA) [16,17] networks. ER networks are characterized by a degree distribution that peaks at an average and decays exponentially for large degrees, while BA networks reproduce a power-law degree-distributed network with exponent 3, by incorporating two ingredients common to real networks: growth and preferential attachment.

Our results show that, in the absence of resource constraints, a positive correlation results in a lower epidemic threshold than a negative correlation does for both coupled ER and BA networks. This is in agreement with previous studies showing that a positive correlation increases the robustness of the network and, thus, results in better connectivity [4–6]. However, in the presence of constraints, the result is qualitatively different: in both network types the epidemic threshold obtained through a positive correlation is higher than the one obtained through a negative correlation: intersimilar coupled networks spread less efficiently than negatively correlated networks in the presence of constraints. As a consequence of these results we suggest that future work must account for real-world limitations when considering coupled networks.

II. CONSTRAINED EPIDEMIC SPREADING MODEL

For simplicity and clarity of the results, we consider only the two extreme cases of maximally positive and maximally negative correlations. Imperfect correlation can be considered, for example, by coupling a fraction of the nodes in a maximally correlated manner, and the rest in an uncorrected manner, as done in [4]. In order to construct a maximally positively (negatively) correlated coupled network, we sort the nodes according to their degree and match two nodes from each network in order (in opposite order) of the degree rank [4,6]. Note that in a duplex system the degree of a node is the sum of the degrees in each network minus the number of overlapping links in the two networks, which can be neglected in the limit $N \to \infty$ for random, sparse networks with the largest degree of, at most, order $\sqrt{(}N)$ [4], where N is the number of nodes in the network. Therefore, the degree correlation between coupled nodes affects the connectivity of the obtained duplex and can introduce higher order correlations such as degree-degree correlations [4]. Generally, degree-correlated coupling does not necessarily imply degree-degree correlations in the obtained system of coupled networks. While degree-correlated coupling accounts for the correlation between the degrees of coupled nodes in the different networks, degree-degree correlation accounts for the correlation between the degrees of nodes connected by an edge. For example, in the case of maximally correlated coupled ER networks with the same degree distribution, the degree-degree correlation in the obtained multiplex is close to 0 [4]. Finally, in order to distinguish between the effects of constraints and correlated coupling, we also consider uncorrelated coupled networks where nodes are randomly coupled.

Given a coupled network, which we call the *original graph*, and an *interaction limit* m, we proceed as follows. At each time step we construct an *interaction graph* by successively selecting a node at random from the original graph that has not yet reached its interaction limit and randomly choosing one of this node's neighbors that has also not reached its own interaction limit. We continue until no interactions can be added. To prevent the first nodes from exhausting their interaction limit early we shuffle the node order before each selection. The choice of neighbors with which to interact is made independently of their epidemic state S, I, or R. Given this interaction graph we update the state of each node, with susceptible nodes with infected neighbors becoming infected with a probability λ and infected nodes recovering at a rate μ.

III. SIMULATION

We consider a duplex consisting of either two ER or two BA networks of size $N = 10^5$ and average connectivity $\langle k_1 \rangle = \langle k_2 \rangle = 6$. We first consider interaction limits m ranging from 10 to 14, which is two links less or more than the mean degree of the duplex, $\langle k \rangle = 12$. Later, we also examine how changing the interaction limit from 0 to 100, while keeping the infection rate constant, affects the results.

Without loss of generality we set the recovery rate to unity, $\mu = 1$, as different recovery rates can be considered by a proper rescaling of λ, m, and time. Note that at this point we assume

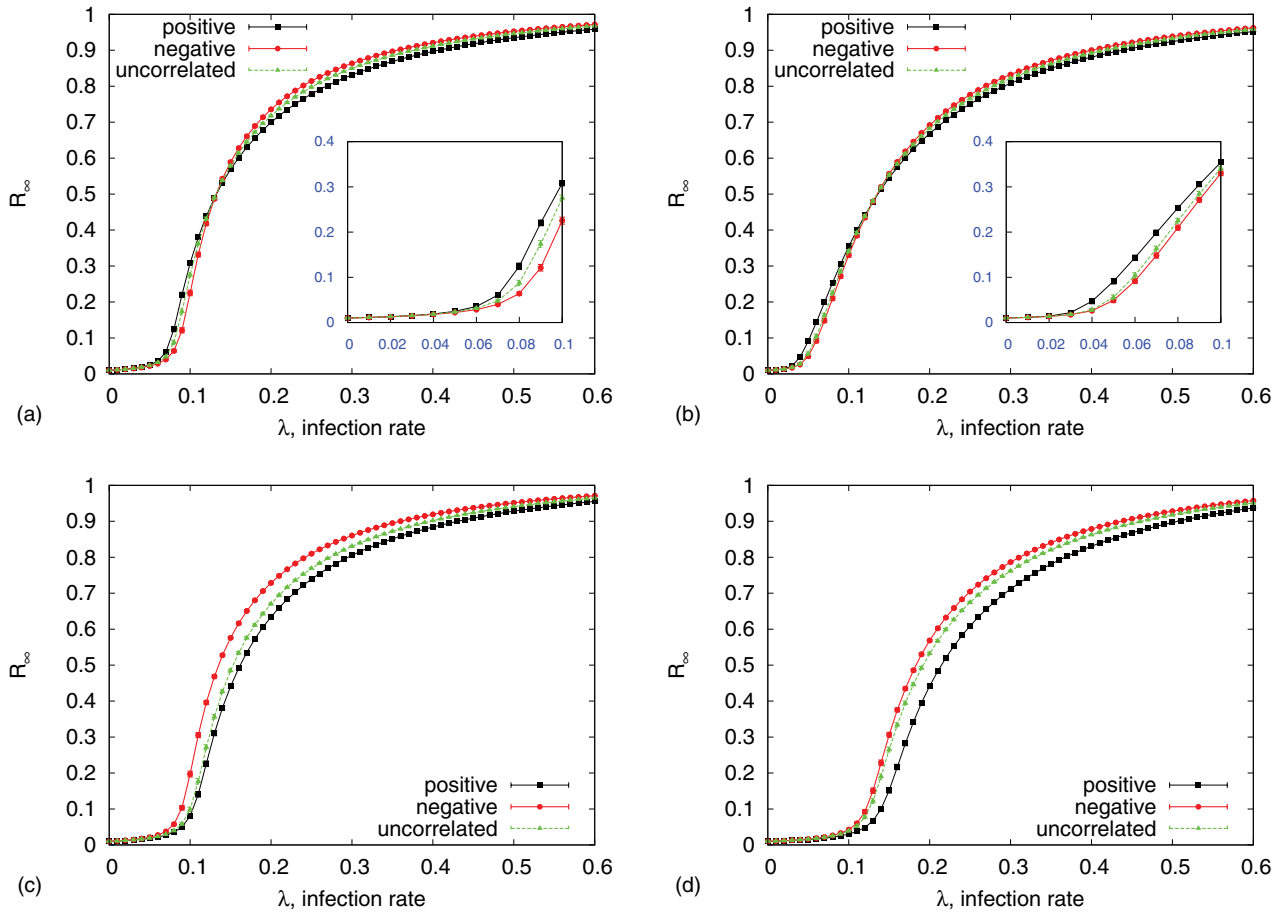

FIG. 1. (Color online) Fraction of infected nodes at the end of the epidemic outbreaks R_∞ as a function of the infection rate λ for constrained and nonconstrained epidemic spreading, running in a positively correlated [(black) squares], negatively correlated [(red) circles], and uncorrelated [(green) triangles] network consisting of two ER or BA networks of size $N = 10^4$ and mean degree 6. Symbols and error bars (if larger than the symbol size) correspond to the mean and standard deviation computed over 1000 simulation runs. (a) Nonconstrained epidemic in coupled ER networks. (b) Nonconstrained epidemic in coupled BA networks. (c) Constrained epidemic with interaction limit $m = 12$ in coupled ER networks. (d) Constrained epidemic with interaction limit $m = 12$ in coupled BA networks.

that the interaction limit and the disease are taking place on the same time scale, i.e., both are carried out using the same discrete time steps of length Δt, which in our simulation is $\Delta t = 1$. The more general case of separate time scales might also be addressed by an appropriate rescaling of m. For example, in the case of a disease evolving over months though a population limited to meeting a certain number of friends in a week, the interaction limit can be rescaled in order to obtain the number of friends a person is limited to meet in a month. However, this rescaling is not always possible and depends on the nature of the dynamics. We performed 1000 simulation runs, our results obtained by averaging over 100 random starting configurations, on 10 different realizations of the random networks.

The mean-field approximation for the epidemic threshold in the thermodynamic limit $N \to \infty$ is given by

$$\lambda_c = \frac{\langle k \rangle}{\langle k^2 \rangle}, \tag{1}$$

where $\langle k \rangle$ and $\langle k^2 \rangle$ are the first and second moments of the network degree distribution, respectively [18]. The epidemic threshold is the critical infection rate in which higher infection rates $\lambda > \lambda_c$ result in a finite fraction of infected nodes and lower infection rates $\lambda < \lambda_c$ result in an infinitesimally small number of infected nodes in the limit of very large networks. Networks with strongly fluctuating connectivity distributions, like scale-free networks, show a vanishing epidemic threshold for increasing network sizes, $\langle k^2 \rangle \to \infty$ for $N \to \infty$. However, real-world networks always have a finite size and thus an effective threshold [18].

In Fig. 1 we show the fraction of recovered nodes at the end of an epidemic outbreak R_∞ as a function of the infection rate λ in the cases of constrained and regular epidemic spreading, starting with a fraction of 0.01 infected node. Symbols and error bars (where shown) correspond to the mean and standard deviation computed over 1000 simulation runs; where error bars are not shown, they would be smaller than the symbol size. We can see that in the cases of regular nonconstrained epidemic spreading [Figs. 1(a) and 1(b)], the curve for a positive correlation [(black) squares] goes up earlier than the curve for a negative correlation [(red) circles] for both ER and BA networks. In other words, the

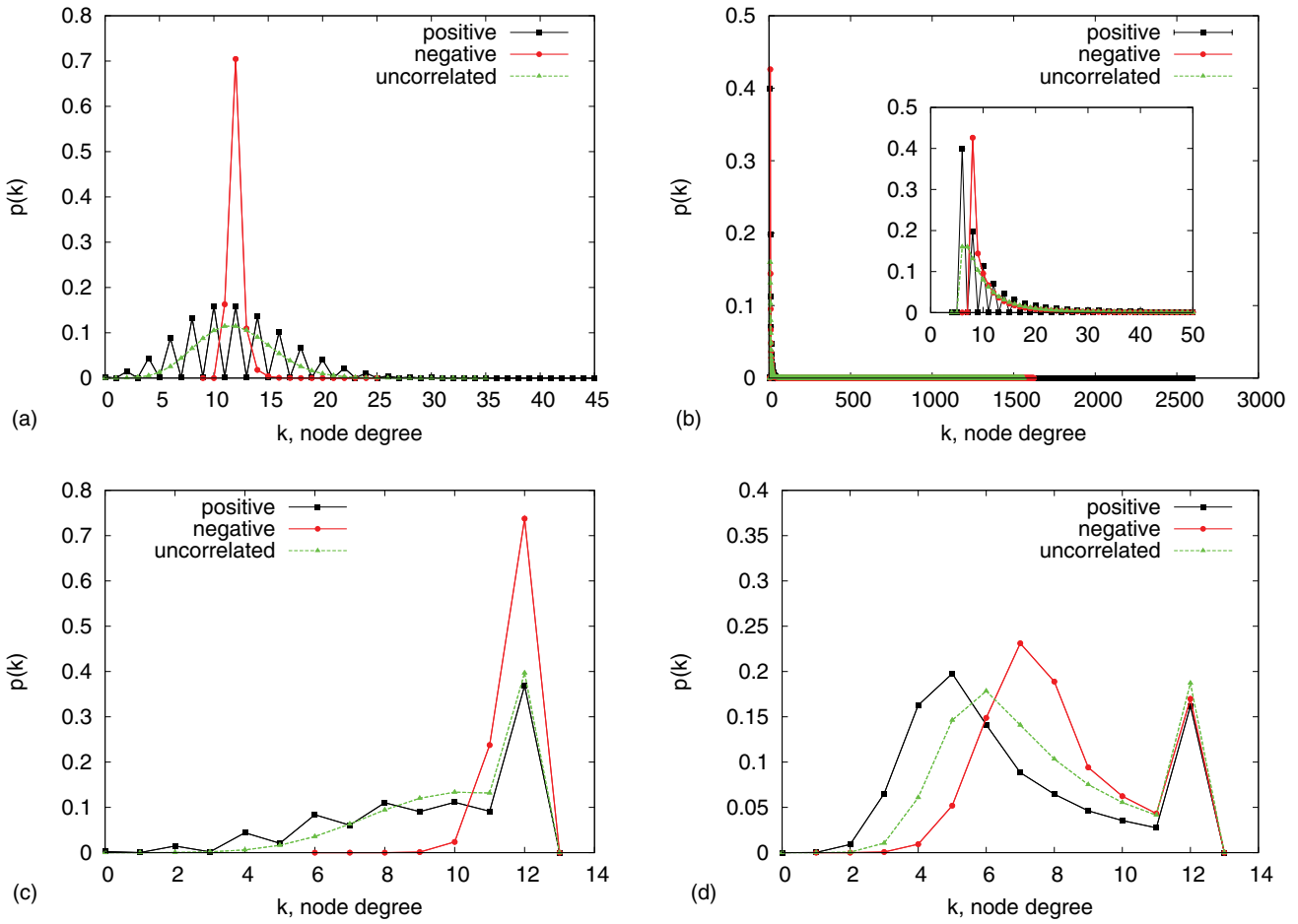

FIG. 2. (Color online) Degree distributions of the original and the interaction graphs, obtained from a positively correlated [(black) squares], a negatively correlated [(red) circles], and an uncorrelated [(green) triangles] network consisting of two ER or BA networks of size $N = 10^4$ and mean degree 6. Results obtained by averaging all the graphs. (a) Original graphs of coupled ER networks. (b) Original graphs of coupled BA networks. (c) Interaction graphs with interaction limit $m = 12$ obtained from coupled ER networks. (d) Interaction graphs with interaction limit $m = 12$ obtained from coupled BA networks.

epidemic threshold of positively correlated coupled networks is lower than that for the negatively correlated case. If we define the epidemic threshold as the highest infection rate in which $R_\infty < 0.1$, then we obtain from the simulation that the epidemic threshold for positively correlated coupled networks is $\lambda_c \approx 0.07$ for ER and $\lambda_c \approx 0.05$ for BA, while that for negatively correlated networks is $\lambda_c \approx 0.08$ for ER and $\lambda_c \approx 0.06$ for BA.

However, in the case of constrained epidemic spreading with interaction limit $m = 12$ [Figs. 1(c) and1(d)], we see that positively correlated ER and BA networks exhibit higher epidemic thresholds ($\lambda_c \approx 0.1$ and $\lambda_c \approx 0.14$, respectively) than in the negatively correlated cases ($\lambda_c \approx 0.08$ and $\lambda_c \approx 0.12$, respectively). Finally, in the case of regular epidemic spreading [Figs. 1(a) and 1(b)], once the infection rate is higher than the threshold, it grows more abruptly in the negative-correlation case than in the positive case (the red curve crosses the black curve and stays above it). This result agrees with earlier work [4,6] showing that the giant component in a positively correlated multiplex emerges at lower link densities than for the negatively correlated multiplex but, once formed, grows much more gradually. As expected, in all four figures, the curve with (green) triangles, representing uncorrelated networks, is between the curve with (red) circles and the curve with (black) squares. However, uncorrelated coupled ER networks behave more similarly to positively correlated coupled ER networks, where for BA networks it is the opposite. This is a result of the obtained degree distributions when coupling ER or BA networks.

In the following we examine the degree distributions of the original and interaction graphs obtained from the simulation. Recall that the original graph is the duplex consisting of two random networks, and interactions take place by constraining the maximum number of neighbors in the original graph with which a node can interact at each time step. By substituting the first and second moments obtained from the simulation in Eq. (1), we can approximate the epidemic threshold shown earlier.

Figure 2 shows the degree distributions obtained by averaging over all the original and interaction graphs. The original graphs of positively correlated networks display a zigzag pattern originating in the fact that, for large enough

networks ($N \to \infty$), each node has exactly the same degree in both networks [4]. We can see that the original graph consisting of uncorrelated coupled ER networks behaves more similarly to the positively correlated original graph than the negatively correlated one. This is due to the narrow degree distribution of a single ER network, where most of the nodes have a degree close to the mean (6 in this case). Therefore, when the nodes are coupled in a negatively correlated manner, there is a a very large peak at the mean degree of the duplex (12 in this case). However, uncorrelated or positively correlated coupling gives a higher chance of degrees farther away from the mean being obtained, resulting in a broader degree distribution. In the case of BA networks, the opposite process occurs: as the degree distribution of a single BA network is broad, positively correlated coupling gives rise to very high degrees that have a very small chance of being obtained in the case of negatively correlated and uncorrelated coupling.

By introducing a constraint on a network we narrow its degree distribution, reducing the high fluctuations in connectivity. Therefore, networks with a narrow degree distribution in the first place (as the negatively correlated original graph) are less affected by this process. However, we also cut more links by applying a constraint on a positively correlated network as it has more high-degree nodes, thus decreasing its mean degree [the numerator in Eq. (1)]. However, the decrease in the second moment is more significant, resulting in original moments for the ER networks of $\frac{\langle k\rangle}{\langle k^2\rangle} \approx \frac{12}{168.08} = 0.071$ for positively correlated networks and $\frac{\langle k\rangle}{\langle k^2\rangle} \approx \frac{12}{144.46} = 0.083$ for negatively correlated ones. After application of the constraint, the new values are $\frac{\langle k\rangle}{\langle k^2\rangle} \approx \frac{9.51}{97.21} = 0.098$ for positively correlated networks and $\frac{\langle k\rangle}{\langle k^2\rangle} \approx \frac{11.82}{139.94} = 0.084$ for negatively correlated ones. In both constrained and regular epidemic spreading in a duplex of ER networks, the mean field gives a good approximation of the values obtained from the numerical simulation, yielding an epidemic threshold of $\lambda_c \approx 0.07$ and $\lambda_c \approx 0.08$ for regular epidemic spreading and of $\lambda_c \approx 0.1$ and $\lambda_c \approx 0.08$ for constrained epidemic spreading in positively and negatively correlated networks, respectively. Also, the values obtained from the simulation and the approximation both show a small difference between constrained and nonconstrained epidemic spreading in negatively correlated coupled ER networks. The reason is that most of the nodes in a duplex of negatively correlated ER networks have a degree equal to or less than 12, which is the interaction limit. Therefore, the constraint does not affect most of the nodes, and a similar epidemic threshold is obtained.

In the case of regular epidemic spreading in a duplex of BA networks, although qualitatively in agreement, the values obtained from simulation, $\lambda_c \approx 0.05$ and $\lambda_c \approx 0.06$, deviate from those obtained by Eq. (1), $\frac{\langle k\rangle}{\langle k^2\rangle} \approx \frac{11.99}{564.26} = 0.021$ and $\frac{\langle k\rangle}{\langle k^2\rangle} \approx \frac{11.99}{339.45} = 0.035$ for positively and negatively correlated networks, respectively. In the case of constrained epidemic spreading in coupled BA networks, the values obtained from the mean-field approximation are $\frac{\langle k\rangle}{\langle k^2\rangle} \approx \frac{6.85}{55.37} = 0.123$ and $\frac{\langle k\rangle}{\langle k^2\rangle} \approx \frac{8.3}{73.53} = 0.11$ for positively and negatively correlated networks, respectively. These values are closer (especially for the negative correlation) to the values obtained from the simulation: $\lambda_c \approx 0.14$ and $\lambda_c \approx 0.12$ for positively and negatively correlated networks, respectively.

In order to explain these differences, we examine the effect of degree-correlated coupling and an interaction limit on the degree-degree correlations of the obtained original and interaction graphs. As mentioned before, degree-degree correlation is the tendency of nodes to **connect** with similar-degree nodes, where degree-correlated coupling is the tendency of nodes to **couple** with similar-degree nodes. We use both the nearest-neighbors average connectivity (NNAC) curve [19] and the Pearson correlation coefficient of the degrees of nodes at either end of a link in the duplex [20] as a measure of degree-degree correlation. Figures 3(a) and 3(b) show the NNAC curves obtained for the original graphs (only correlated or uncorrelated coupling, no interaction limit) consisting of ER and BA networks, respectively. In the case of coupled ER networks [Fig. 3(a)], all three curves show almost no degree-degree correlations. This is also confirmed by the Pearson correlation coefficients obtained: $-5.288 \times 10^{-5} \pm 0.0013$, $4.346 \times 10^{-5} \pm 0.0012$, and $-2.236 \times 10^{-5} \pm 0.0012$ for positively correlated, negatively correlated, and uncorrelated ER networks, respectively. This result is in agreement with [4], showing that the positive degree-degree correlations of a multiplex network consisting of two correlated coupled ER networks vanish at $\langle k_1\rangle = \langle k_2\rangle$, which is exactly what happens in our simulation. The nonconstrained original graph consisting of two BA networks displays a degree-degree correlation very similar to the one obtained for the single BA network (Fig. 4): the NNAC curve shows power-law dependence, in agreement with [21], while the Pearson correlation coefficient (-0.02 ± 0.001, -0.013 ± 0.001, -0.017 ± 0.0014, and -0.018 ± 0.002 for positively correlated, negatively correlated, and uncorrected duplexes and a single BA network, respectively) is close to 0, in agreement with [20]. The power-law behavior of the NNAC curve might explain the deviation from the mean-field approximation, as the approximation neglects the connectivity correlations in the network.

Figures 3(c) and 3(d) show the NNAC curves obtained for the interaction graphs constrained by interaction limit $m = 12$ consisting of ER and BA networks, respectively. Pearson correlation coefficients obtained are -0.055 ± 0.001 and -0.34 ± 0.002 in the case of positively correlated ER and BA networks, respectively, and -0.002 ± 0.001 and -0.12 ± 0.001 in the case of negatively correlated ER and BA networks, respectively. In the cases of both ER and BA networks, positively correlated graphs exhibit stronger negative degree-degree correlations than negatively correlated graphs. This is due to the construction of the interaction graph, which creates a tendency for high-degree nodes to have lower-degree nodes as neighbors and has a stronger effect on a broad degree distribution: In order to have a degree closer to the interaction limit, a node needs its neighbors not to reach their limit before it chooses to interact with them. As lower degree nodes have fewer neighbors with which to interact, they "wait" to interact with the node. By analogy, a person whose friends are high-degree nodes might want to meet them at the end of the week but might find they are too tired since they have met many friends during the week (they have reached the limit). In contrast, the individual's low-degree friends will be

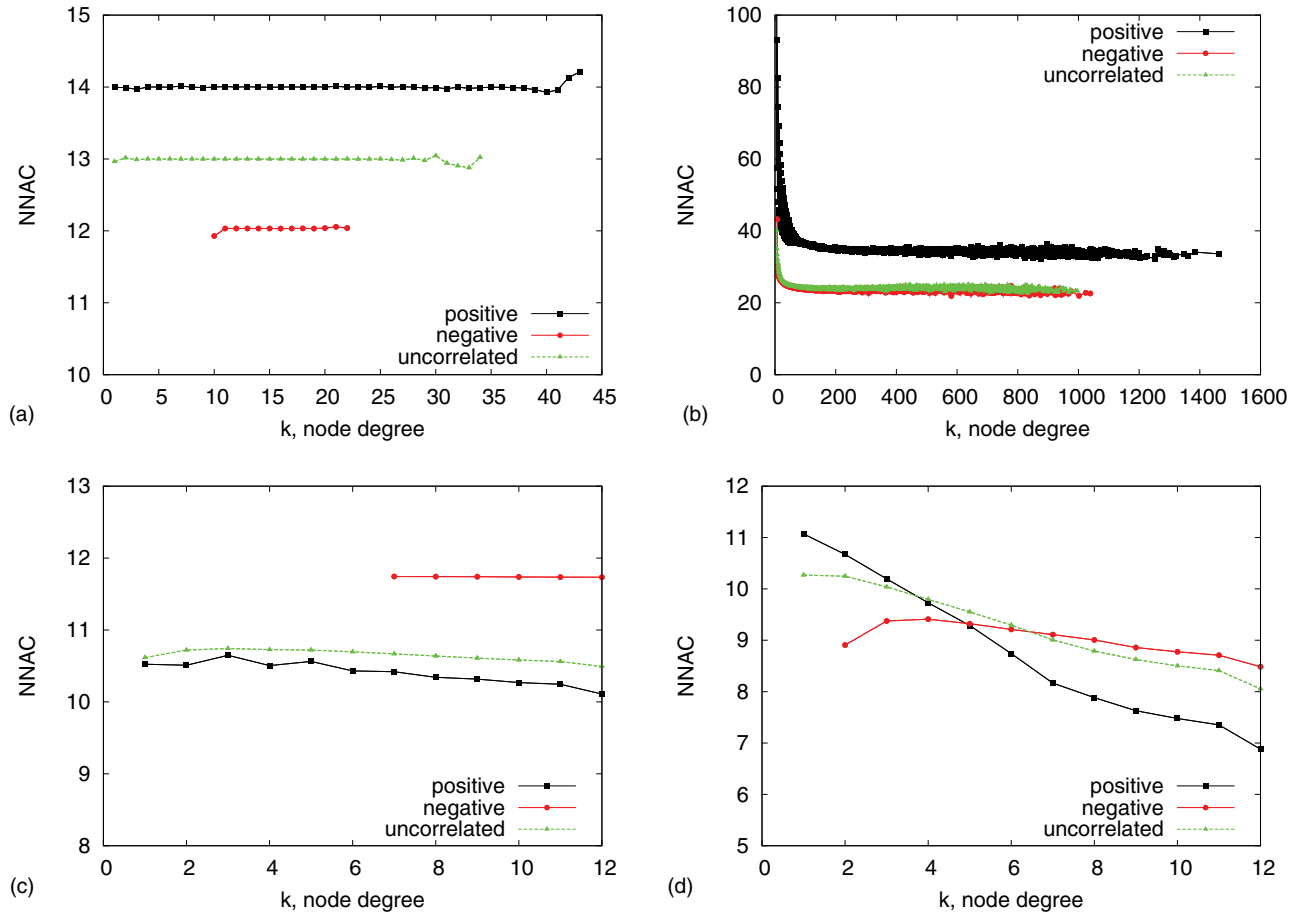

FIG. 3. (Color online) Nearest-neighbors average connectivity (NNAC) as a function of node degree for a positively correlated [(black) squares], a negatively correlated [(red) circles], and an uncorrelated [(green) triangles] network consisting of two ER or BA networks of size $N = 10^4$ and mean degree 6. Results obtained by averaging all the graphs. (a) Original graphs of coupled ER networks. (b) Original graphs of coupled BA networks. (c) Interaction graphs with interaction limit $m = 12$ obtained from coupled ER networks. (d) Interaction graphs with interaction limit $m = 12$ obtained from coupled BA networks.

happy to meet him or her since they have not yet exhausted their limits. This process produces stronger degree-degree correlation in cases where the original graph has a broad degree distribution, as in the case of positively correlated BA networks. And indeed, the deviation of the simulation values from the mean-field approximation is more significant in the case of constrained epidemic spreading in positively correlated BA networks (0.14 vs 0.123) than in the case of negatively correlated BA networks (0.12 vs 0.11). The uncorrelated case, as in previous figures, behaves more similarly to the positively correlated case for ER networks, and the opposite for BA networks.

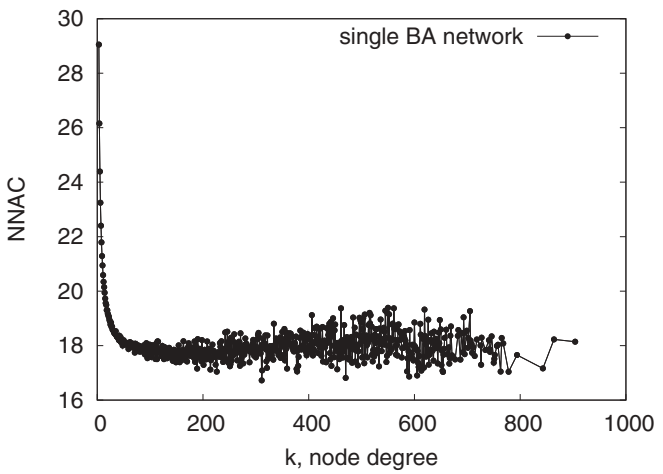

FIG. 4. Nearest-neighbors average connectivity (NNAC) as a function of node degree for a single BA network of size $N = 10^4$ and mean degree 6. Results obtained by averaging all the graphs.

Finally, we examine how changing the interaction limit m affects the results. Until now we have used an interaction limit of $m = 12$. In Fig. 5, we show R_∞, the fraction of recovered nodes at the end of the epidemic outbreaks, as a function of m, where $\lambda = 0.1$. Both graphs start with the curve with (red) circles (corresponds to negative coupling) above the curve with (black) squares (positive coupling), which means that negatively correlated coupled ER and BA networks result in a larger number of infected nodes using the same interaction limit and the same infection rate. At some point, $m = 17$ in the case of ER and $m = 55$ in the case of BA, the curves cross each other, and afterwards the positively correlated networks become more efficient in spreading the epidemics.

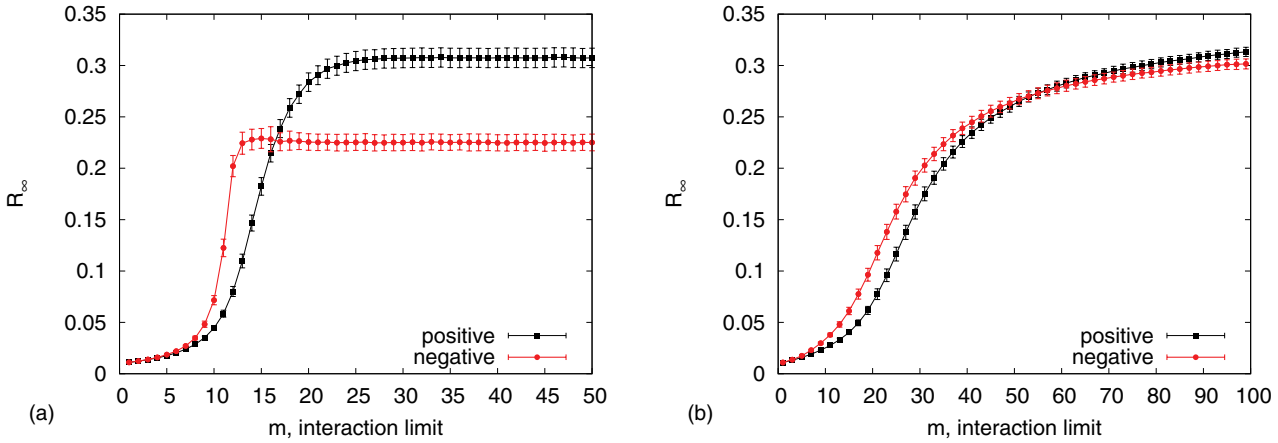

FIG. 5. (Color online) Fraction of infected nodes at the end of the epidemic outbreaks R_∞ as a function of the interaction limit m for constrained epidemic spreading at infection rate $\lambda = 0.1$, running in positively [(black) squares] and negatively [(red) circles] correlated networks consisting of two ER or BA networks of size $N = 10^4$ and mean degree 6. Symbols and error bars (if larger than the symbol size) correspond to the mean and standard deviation computed over 1000 simulation runs. (a) Coupled ER networks; (b) Coupled BA networks.

This means that the interaction limit no longer impedes the spread of the epidemic: it is sufficiently high not to function as a limit *per se* and does not limit nodes' interactions in the network.

IV. SUMMARY

We have considered the effect of constraining the number of interactions a node can have at each time step of a SIR epidemic spread running in a correlated coupled network consisting of two random networks sharing the same set of nodes. We have shown that, in contrast with recent studies, positively correlated coupled networks are less efficient in spreading the epidemic than negatively correlated networks in the presence of constraints. We obtained an epidemic threshold $\lambda_c \approx 0.1$ for positive correlations and $\lambda_c \approx 0.08$ for negative correlations in the case of two ER networks and $\lambda_c \approx 0.14$ and $\lambda_c \approx 0.12$ for positively and negatively correlated coupled BA networks, respectively. However, when considering "regular" nonconstrained SIR epidemic spreading, our results agree with previous studies showing that a positive correlation increases the connectivity of the overall network. We obtain epidemic thresholds $\lambda_c \approx 0.07$ and $\lambda_c \approx 0.08$ for positively and negatively correlated coupled ER networks, respectively, and $\lambda_c \approx 0.05$ and $\lambda_c \approx 0.06$ for positively and negatively correlated coupled BA networks.

By obtaining a qualitatively different result when considering constraints, we illustrate the importance of incorporating more realistic scenarios in future models for coupled complex networks. In the future we would like to examine the effect of failures in these models. This issue is particularly interesting when considering failure probability inversely proportional to the degree of a node. This is a realistic assumption, since important (high-degree) nodes are usually better protected against failures than less important (low-degree) nodes. Finally, as we mentioned earlier, it might be the case that biological networks exhibit closer-to-random internetwork coupling than other networks. We would like to investigate this issue further using more biological data sets.

[1] M. Kurant and P. Thiran, Phys. Rev. Lett. **96**, 138701 (2006).
[2] S. V. Buldyrev, R. Parshani, G. Paul, H. E. Stanley, and S. Havlin, Nature **464**, 1025 (2010).
[3] E. A. Leicht and R. M. D'Souza, arXiv:0907.0894.
[4] K.-M. Lee, J. Y. Kim, W.-k. Cho, K.-I. Goh, and I.-M. Kim, New J. Phys. **14**, 033027 (2012).
[5] R. Parshani, C. Rozenblat, D. Ietri, C. Ducruet, and S. Havlin, Europhys. Lett. **92**, 68002 (2010).
[6] W.-k. Cho, K.-I. Goh, and I.-M. Kim, arXiv:1010.4971.
[7] S. V. Buldyrev, N. W. Shere, and G. A. Cwilich, Phys. Rev. E **83**, 016112 (2011).
[8] R. M. Anderson and R. M. May, in *Infectious Diseases of Humans* (Oxford University Press, New York, 1992).
[9] V. Colizza, A. Barrat, M. Barthélemy, and A. Vespignani, Proc. Natl. Acad. Sci. USA **103**, 2015 (2006).
[10] Y. Moreno, M. Nekovee, and A. F. Pacheco, Phys. Rev. E **69**, 066130 (2004).
[11] D. H. Zanette, Phys. Rev. E **65**, 041908 (2002).
[12] A. L. Lloyd and R. M. May, Science **292**, 1316 (2001).
[13] S. Wasserman and K. Faust, in *Social Network Analysis: Methods and Applications* (Cambridge University Press, Cambridge, 1994).

[14] P. H. Thrall, J. Antonovics, and D. W. Hall, Am. Nat. **142**, 543 (1993).
[15] P. Erdős and A. Rényi, Publ. Math. Inst. Hung. Acad. Sci. **5**, 17 (1960).
[16] A.-L. Barabási and R. Albert, Science **286**, 509 (1999).
[17] A.-L. Barabási, R. Albert, and H. Jeong, Physica A **272**, 173 (1999).
[18] Y. Moreno, R. Pastor-Satorras, and A. Vespignani, Eur. Phys. J. B **26**, 521 (2002).
[19] R. Pastor-Satorras, A. Vázquez, and A. Vespignani, Phys. Rev. Lett. **87**, 258701 (2001).
[20] M. E. J. Newman, Phys. Rev. Lett. **89**, 208701 (2002).
[21] A. Vázquez, R. Pastor-Satorras, and A. Vespignani, Phys. Rev. E **65**, 066130 (2002).